

Antimicrobial and anticorrosive efficacy of inorganic nanoporous surfaces

M. C. Connelly¹ · G. S. Reddy¹ · Mallikarjuna N. Nadagouda² · J. A. Sekhar^{1,3}

Received: 30 May 2016 / Accepted: 22 August 2016 / Published online: 14 September 2016
© Springer-Verlag Berlin Heidelberg 2016

Abstract The relationship between microbe populations that are active on engineered-product surfaces and their relationship to surface corrosion or human health is increasingly being recognized by the materials engineering community as a critically important study-direction. Microbial contamination from biofilms and germ colonies leads to costs that are reported to be extremely high every year in infection control, epidemics, corrosion loss and energy/infrastructure materials loss throughout the world. Nanostructured surfaces, particularly those that are hard-surface nanoporous (pore radii between 2 and 1000 nm), are an emerging class of surfaces that have recently been recognized as important for the prevention of microbial colony growth and biofilm formation. Such nanostructured/nanoporous surfaces, whether made with deposited nanoparticles (welded nanoparticles), or formed by ion-assisted growth on a surface have been found to display biocidal activity with varying efficacy that depends on both the microbe and the nanosurface features. The rate of mortality from common pathogens that are resident in ubiquitous bio-films when attached to common engineering surfaces made of steels, titanium and zirconium appears to be increasing. In this short review, we look at methods of manufacture of durable (i.e., highly scratch resistant) nanostructuring on commonly used engineering surfaces. The microstructures, energy dispersive X-ray analysis,

X-ray photo-electron spectroscopy and other types of characterization of a few such surfaces are presented. Simple tests are required by the surface engineering community for understanding the efficacy of a surface for antimicrobial action. These are reviewed. The surface drying rate and the dynamics of the droplet spread have been proposed in the literature as quick methods that correlate well with the residual antimicrobial activity efficacy even after some surface abrasion of the nanostructured surface. A categorization of a surface against short-term antimicrobial action and long-term action is proposed in this review article. Test periods that span time-frames greater than 5 years have demonstrated a high efficacy of the nanoporous nanostructures for preventing bio-film formation. New comparative results for diamond- and graphite-containing surfaces are presented. A brief discussion on a recently developed plasma application technique for creating durable nanoporous surfaces is presented. Although considerable information is now available regarding tunable surface nanofeatures for antimicrobial efficacy, there is a need for more research activity, particularly directed toward the low cost manufacture and rapid characterization of durable (wear and chemical resistant) surfaces that display permanent antimicrobial behavior.

Keywords Engineered nanostructured nanoporous surfaces · Antibacterial surface · Antimicrobial · Top-soil bacteria · Surface scratch tests · Plasma processing methods

✉ J. A. Sekhar
j.sekhar12@yahoo.com

¹ Thermodynamics and Design Institute, MHI Inc., 750 Redna Terrace, Cincinnati, OH 45215, USA

² Department of Mechanical and Materials Engineering, Wright State University, Dayton, OH 45324, USA

³ University of Cincinnati, Cincinnati, OH 45221, USA

Introduction

The scientific understanding of the adhesion, formation, prevention and inactivation of biofilms on commonly used engineering surfaces is critical for public health as well as

for the materials economy. Nanoporous and nanostructured surfaces are being considered for use as surface chemical reservoirs of antimicrobial materials or even for their direct biocidal action without the need for added chemicals. Nanostructured surfaces are often antimicrobial (i.e., prevent growth of bacteria or inactivate other microbes) because of direct topological (curvature) action and/or from their enhanced chemical activity (chemistry) in influencing antibacterial surface properties. Microbes and biofilms resident on common engineering surfaces, such as stainless steel, can lead to the spread of disease or significantly impact the corrosion behavior of a surface (Reddy et al. 2012; Fontana and Green 1967; Örnek et al. 2002). Corrosion and nosocomial activity are known to be the cause of significant financial and energy loss every year as any similar search phrase query in the web will reveal. Microbial contamination from biofilms leads to more than \$300 billion costs throughout the world in infection control (Santos et al. 2016; Chung et al. 2007; Mayhall 1999), epidemics (Michels et al. 2009; Noyce et al. 2007; Setlow 2006), corrosion (Noyce et al. 2006; Kobrin 1993; Heitz et al. 1996; Videla 1996; Javaher 2008; Rao et al. 2000), and energy and infrastructure material loss yearly (Starosvetsky et al. 2001; Emerson and Moyer 1997; Finneran et al. 2003; Moeseneder et al. 1999; Hamilton 1985). Surface colonization and biofilm formation, even in laboratory conditions, happen within a few months and seemingly does not require a long gestation period (Reddy et al. 2012). Bacterial-assisted corrosion occurs on metallic as well as nonmetallic surfaces (ceramic and PVC pipes) with or without the presence of atmospheric oxygen (Dai et al. 2000; Liao et al. 2010; Rao et al. 2000). Corrosion can be highly penetrative. The problems from bacterial corrosion may also, thus, impact the bulk material along with the surface (Hicks 2009; Finneran et al. 2003; Graff and Seifert 2005; Keough et al. 2003). In this review, it will be noted that antibacterial and antifungal efficacies are interchangeable where it pertains to the efficacy of preventing growth.

Bacterial corrosion is a type of corrosion promoted by chemoautotrophs, e.g., bacteria, which use the corrosion process to exchange energy. Biofilms are often associated with specific bacterial corrosion. Biofilms are also associated with a broad range of problems in the areas of drinking water distribution systems, industrial water supply systems, biomaterials and implant-related infections. Several novel surface engineering methods including those of creating *hard* scratch resistant nanoporous surfaces are being explored for antimicrobial surface engineering uses (Ksoll et al. 2007; de la Fuente et al. 2010; Marsh et al. 2005; Moeseneder et al. 1999; Rahman et al. 2007; Reddy et al. 2012). For example, a reservoir for the loading and release of bactericidal silver-based quaternary chemicals (Li et al.

2006) in pores with a nanoparticle surface cap containing immobilized bactericides has been proposed by an aqueous layer-by-layer deposition technique. Titanium oxide surfaces are known to very antibacterial and highly anti-infectious (Visai et al. 2011; Ketabchi et al. 2016; Losic and Santos 2015). Although the mechanism of electron availability through photo-catalysis of CO₂ and H₂ is thought to be mainly operative for antibacterial activity, there is scope for a better assessment of the mechanisms that involve such redox reactions (Cafun et al. 2013). This is also true for the NO₂ and hypotonic mechanisms sometimes attributed to antimicrobial surface behavior (Reddy et al. 2012). Other mechanisms have been discussed by Visai et al. (2011).

Nanoporous surfaces are fairly ubiquitous. Such surfaces can display a wide range of morphologies for the phases and pores. For the purposes of this review, nanopores are defined as pores with a radii between about 2 and 1000 nm (i.e., including the class, mesopores but smaller than micropores). A more narrow range that is sometimes attributed to nanopores is 10–500 nm. A few examples of commonly noted phase morphologies (shapes), the typical bimodal-distributions and the size-range of nanopore features that have been reported on various surfaces are shown in Fig. 1. Although clearly not comprehensive of all distribution in the range, a reasonably large variety is captured in the figure. The two key properties that are discussed in this article are (1) the adherence of the nanostructure with a denser substrate and (2) the ability of the surface to display biocidal or bacteriostatic behavior (i.e., prevent or delay the growth of bacterial colonies and/or biofilms). The complete mechanical structural assessment of ductile nanoporous surface structures, especially those that contain nonmetallic nanoparticles, requires a rigorous fracture toughness of the kind proposed by Li et al. (1992). However, an easier and quicker test which is now generally accepted is the ASTM scratch test which is described below.

A range of antimicrobial efficacy ranging from mild efficacies, like disinfection, to large log-reduction treatments like sterilization appears to be possible from nanoporous surfaces (Table 1). Efficacy comparison may be made with soaps, detergents, alcohol and superheated-steam-based antimicrobial methods. Several techniques have been reported in the literature for obtaining antimicrobial nanostructured surfaces (Tiller et al. 2001; Locklin 2011; Child 2006; Atha et al. 2012). However, this review is mostly concerned with durable nanostructuring and methods for obtaining such durable nanosurfaces (Burada et al. 2014; Bacakova and Svorcik 2008; Cvetkovic et al. 2010; Reddy and Sekhar 2016; Reddy et al. 2012, 2015a, b; Yuan and Pehkonen 2009). This review does not contain information on the use of dissolvable paints, creams or resins which can also sometimes contain soft nanoparticles or biocidal chemicals (Lane 1991; Setlow 2006; Cortezzo et al. 2004; Coleman and Setlow 2008).

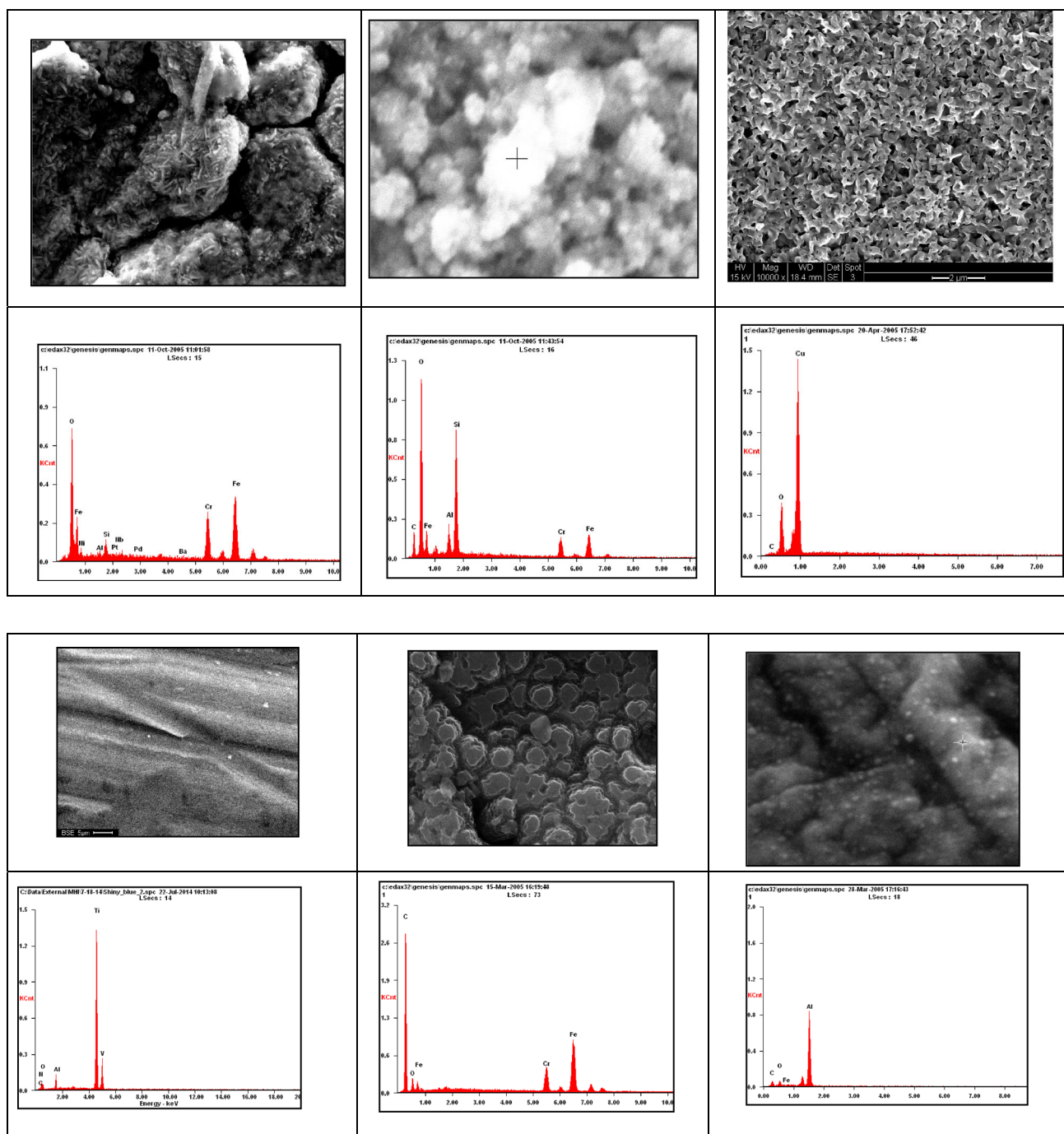


Fig. 1 Collage of a few antibacterial nanoporous surfaces deposited or grown on 316 grade stainless steel by the techniques discussed in references (Reddy et al. 2012, 2015a, b). The compositional analysis by EDAX is shown below each structure. From *top left* to *bottom right* are surface nanostructures of iron/chromium oxides, transition

Bulk nanostructuring has been widely studied and is known to yield materials with unusual properties of extreme strength and magnetic behavior. The methods of manufacture being pursued worldwide include nanostructuring by melt undercooling, vapor deposition and thermo-mechanical deformation strategies that allow very large strains. However,

metal silicides, copper oxide, titanium oxynitride, graphite and diamond on alumina. The *Micron markers* are shown on the photomicrographs. The *top middle column* is $\times 500$, and the *bottom middle column* is $\times 5000$

far less is known about surface nanostructuring. The corrosion and antimicrobial characteristics of nanoporous surfaces are yet to be comprehensively studied. Very few manufacturing techniques are known. It has been suggested that non-equilibrium processing methods will dominate a large part of the next century for development of energy efficient processing

Table 1 Proposed categorization of strong and weak antibacterial surfaces

Class A: Works in a short contact time of less than a few minutes and maintains efficacy in a permanent sense. E.g., durable nanoporous nanostructured, durable oxynitrides, especially for hardy bacteria and high concentrations

Class B: Is non-permanent but offers a significant log reduction. E.g., sterilization

Class C: Works after ~about 24 h. contact time, but is a permanent acting surface. E.g., PVC alcohol treated cleaned surfaces

Class D: Works for less than ~1 h (e.g., coating that is highly soluble)

Class E: Only instantaneous action like a disinfectant or alcohol which works when applied but has no permanency or durability

Class A is strongest, and Class D is weakest. Class E is strong but of limited time efficacy. Please consult <http://www.bayzi.com> for details on steam sterilization and steam disinfection. Dry steam (i.e. high quality steam) is the preferred agent compared to mist or misty sprays.

methods (Sekhar 2015). However, it is important to note that ever since the Bronze-Age, nanostructuring has seemingly been used for making certain types of vessels and mirrors, most likely, for the long-term anticorrosive properties that such alloys displayed. Metallic nanostructural and icosahedral features in ancient bronze alloys have been discovered recently (Sekhar et al. 2015). The ancient mirror alloys were *not* nanoporous. They were dense and surprisingly found to comprise of very diffuse interface nanograins ~5 nm. Inorganic materials whether externally produced or by biomineralization (e.g. magnetite, silanes, oxycompounds) are known to be bioactive (Boccaccini 2016). Nitrogen containing materials are now recognized to be an exciting emerging class materials based on the patent-driving-force assessment technique (Connelly 2012). The strong antimicrobial efficacy of durable hard nanoporous oxynitrides (i.e. containing nitrogen and oxygen) is described further below in this article. Oxynitrides surfaces with silver or silica are relatively easy to form as an additive nanoporous inorganic covering on stainless steels and titanium alloys.

Nanostructured surfaces of the type discussed in this article contain firmly joined nanoparticles that are externally deposited or in situ grown. Such nanostructured surfaces often display chemical and other properties that are significantly different than their counterpart individual nanoparticles of the same element or compound (Reddy et al. 2015a, b, Reddy and Sekhar 2016; Burada et al. 2014). It has been noted in the literature that the XPS peak signatures, when comparing the same chemical species in nanostructured and nanoparticle chemical states, are notably shifted because of the possible variations in the overall electron configurations (Cafun et al. 2013). The nanopores are formed between the particle phases or the nanoparticles may reside between the pores (see Figure 1).

Nanostructured/nanoporous surfaces for antimicrobial and antibiofilm efficacy

A comparison of the efficacy of a few nanoporous structures is shown in Fig. 2. Silver and molybdenum compound surfaces are noted to be particularly effective. The

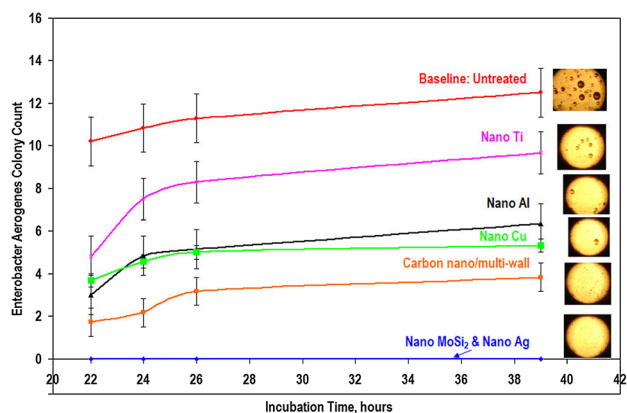
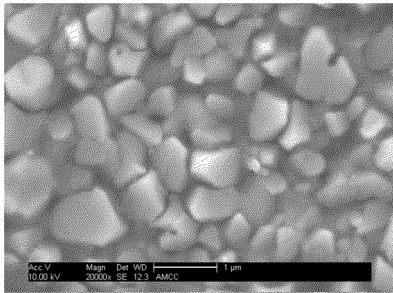
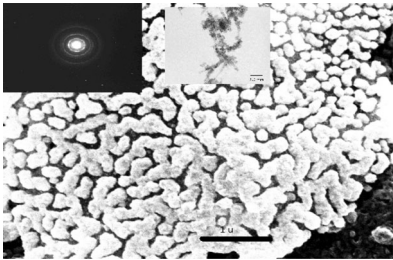


Fig. 2 Comparative efficacy for colony formation on nanostructures of Ag, MoSi₂, C, Cu, Al and Ti From Reddy et al. 2012. Each nanostructure coating was about 500–1000 nm thick applied to a cold rolled 316L stainless steel surface. For comparison, the results from virgin surface of a stainless steel 316L substrate are also shown. The AOAC method described in the text is useful for comparing bacterial colonies. The initial solution concentration was ($\sim 8 \times 10^5$ cfu's/ml) of Gram (–ve) Enterobacter aerogenes. Bacterial colony observations in the petri dish were made from 20 to 39 h of incubation, in accordance with AOAC test procedure 988.18 and 989 (Xu et al. 2011). The swabs from the surfaces were taken after a 2-h contact residence time of the bacterium on the surface

detailed testing methodology and the Gram positive and Gram negative species that were tested on such surfaces are also described further below. New results that compare the efficacy of nanostructured graphite and diamond nanostructures, made from the same starting raw materials, are shown in Table 2. Both these types of surfaces indicate antibacterial efficacy, although the soot-containing (graphitic) surface appeared to be marginally superior. The diffraction patterns and high-resolution TEM indicated that the soot (graphitic) structure is comprised of carbon nanotubes and amorphous particles (see insets in the graphitic nanoporous coating picture).

The determination of antimicrobial efficacy is possible with many types of tests. These include the AOAC test procedure 988.18 and/or 989.11 (AOAC Official Methods of Analysis 1988), ASTM E 2149: Standard Test Method for Determining the Antimicrobial Activity of Immobilized Antimicrobial Agents Under Dynamic Contact Conditions,

Table 2 Enterobacter aerogenes colony formation on inoculated stainless steel surface (control) compared with diamond and graphite nanoporous surface created on similar 316 stainless steel surfaces

Uncoated control	Diamond coated 316 stainless	Amorphous particulate and carbon nanotube-coated 316 stainless
Stainless Steel 316 Grade 50mmx50mmx0.3mm. Polished to ~0.3 micron.		
Microbe contact time on the surface 2 h	Microbe contact time on the surface 2 h	Microbe contact time on the surface 2 h
14-h incubation in petri dish ~ 50 % Dishful area with plenty of colonies ~ 441 Colonies Max. size ~ 0.2 mm ($q = 10$) Remaining all ~ 0.1 mm	14-h incubation in petri dish 31 Colonies Max. size ~ 0.1 mm (all)	14-h incubation in petri dish No colonies
24-h incubation in petri dish ~ 1310 Colonies Max. size ≈ 1.0 mm ($q = 20$) Remaining ≈ 0.4 to 0.8 mm	24-h incubation in petri dish 208 Colonies Maximum size 0.55 mm ($q = 2$) Remaining ≈ 0.3 to 0.5 mm	24-h incubation in petri dish 9 Colonies Maximum size 0.25 mm ($q = 3$) Remaining ≈ 0.2 mm

The table columns from left to right represent the control stainless steel 316 surface (uncoated), diamond nanostructure coated on 316 stainless steel for the middle column and right-most column from the carbon soot-containing coating on 316 stainless steel. The soot structure comprised of amorphous particles and a few single/double wall nanotubes—shown in the two insets, namely the diffraction and TEM photographs. The coatings were about 500 nm—1 micron thick. It is important to mention here that carbon nanotubes are also reported to be toxic (Lam 2004, Service 2004). The nature of nanostructures as far as toxicity and use for antimicrobial use is not yet fully known

JIS Z 2801: Japanese Standard Test for Antimicrobial Product Activity and Efficacy (Japanese Industrial Standard 2005) and the Kirby-Bauer type Zone of Inhibition (ZOI) testing standards, (AATCC-147-2004). In addition, the rapid swab tester results from the Luminester PD-20* are also sometimes used for quick tests (not all tests are recognized by all governments). Table 2, from Reddy et al. 2012, shows the comparison between the efficacies of various nanostructured surface coatings made on a dense stainless steel 316L substrate. The initial solution concentration was ($\sim 8 \times 10^5$ cfu/ml) of Gram (–ve) *Enterobacter Aerogenes*. Bacterial colony observations were made from 20 to 39 h of incubation in the Petri dishes, as per AOAC test procedure 988.18 and 989 (Xu et al. 2011) taken from swabs after a 2-h contact time of the surface and the inoculant species. This residence (contact time) was in a high humidity condition (\sim above 70 %RH relative humidity) for all the test results. Both MoSi_2 and Ag nanostructures effectively prevented colony formation. With the aid of Cincinnati top-soil as the bacterial medium, it was shown that the curvature of surface features plays a

significant role in determining the rate of biocidal activity. The following bacteria were identified in the Cincinnati top-soil: (1) *Arthrobacter Globiformis* (Gram +ve), with morphology of irregular rods and small cocci; (2) *Bacillus Megaterium* (Gram +ve), with morphology of rods, and endospore formation; and (3) *Cupriavidus Necator* (Gram –ve), with morphology of Coccoid and irregular rods (Reddy et al. 2012). Nanostructured/nanoporous surfaces always appear to display antimicrobial efficacy although with varying degrees of efficacy. In reference (Reddy et al. 2012), it was also reported that *E. coli* (ATCC 25922), 1.06×10^9 cfu/ml plated with 1.06×10^4 cells per plates on nanostructured stainless steel and copper substrates, was tested against a virgin stainless steel control substrate in accordance with the JIS Z 2801 protocol (Japanese Industrial Standard 2005) showed the following behavior.

The virgin test plates showed a full 100 %+ to 78.4 % recovery, i.e., essentially no antibacterial activity. The nanostructured surfaces displayed log 2 to log 3 reductions in colonies for the 30-min contact time (such an order of reduction is for example often mandated in food contact

cleaning). Compare with steam use reported in the Baysi site. Nanostructured/nanoporous surfaces are often noted to display strong permanent biocidal activity with varying efficacies that depend on the nanostructure size and chemistry. Silver and Molybdenum disilicide (MoSi_2) were found to be the most effective bactericidal nanostructured agents with MoSi_2 being particularly effective in both low and high humidity conditions (Reddy et al. 2012). Bacteriostatic activity was also recorded in great morphological detail in (Reddy et al. 2012). A resistance to the growth of colonies, even from the simultaneous exposure to diverse bacterial species including *Arthrobacter Globiformis*, *Bacillus Megaterium* and *Cupriavidus Necator* in a topsoil solution with water, was noted in this article. The nanostructure/nanoporous coated stainless steel (S36) killed 98.47 % of the *Staphylococcus aureus* bacteria, while the same bacteria flourished abundantly (757.14 %) in uncoated stainless steel, indicating that the nanostructure coating was capable of killing or inactivating the bacteria. The same structures also showed strong antifungal efficacy (Reddy et al. 2012) The efficacy of a nanostructured surface against colony growth of nonpathogenic bacteria strain ATCC 25922, namely *E-Coli* (Gram-ve) appears to be high regardless of the starting inoculants concentration. The presence of a nanostructured/nanoporous surface was noted to eliminate or delay bacterial colony formation, even with short exposure contact times, and even after simulated surface abrasion (Reddy et al. 2012). It was noted that uncoated

316 stainless steel and copper substrates (controls), i.e., without the nanostructure, always displayed rapid bacterial colony evolution indicating the lack of antimicrobial action. The efficacy of the nanostructured surface against colony formation (bacterial recovery) for *E-Coli* (two strains) and virus Phi 6 Bacteriophage with a host *Pseudomonas syringae* was also studied (Reddy et al. 2012). When comparing antimicrobial efficacy of flat polished surfaces (no curvature or nanostructure feature) against a nanostructure-containing surface (high curvature sometimes from protruding nanoparticles) of the same chemistry, it was clearly noted that bactericidal action resulted from both the nanostructure size and chemistry. Silver and MoSi_2 nanostructures showed very strong bactericidal action for 2 h of contact time for Gram (+ve) *Bacillus Cereus* and Gram (-ve) *Enterobacter Aerogenes*. Other nanoparticles showed a lesser efficacy for the same contact period (Fig. 2). In the case of the top-soil experiments, for a contact time of 2 h, the MoSi_2 appears to indicate significant bacteriostatic action, whereas the silver remained strongly bactericidal, but only in the coated nanoparticle state. With an increase in the contact time prior to colony recognition, the bactericidal increased for nanostructured MoSi_2 top-soil bacteria test conditions. The lag indicates an increase in time during incubation, i.e., in the time prior to noticeable bacterial colony appearance inside a Petri dish at the magnifications of interest of at least 100 \times . A higher lag corresponds to a better inactivation during the contact (Table 2).

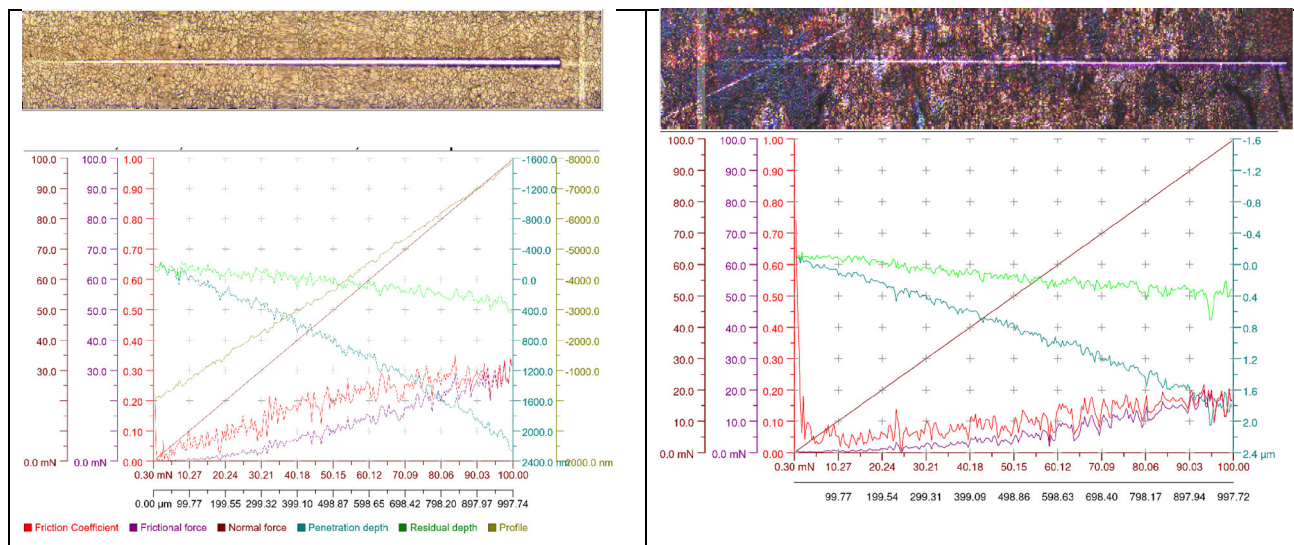


Fig. 3 Features of good scratch-test results from **a** silver nanostructure and **b** molybdenum disilicide nanostructure. The measurement signals are identified and color-coded as follows: Fn: Applied normal load (brown), Pd: Penetration depth during scratch (green), Rd: Residual Depth after scratch (light green), Ft: Frictional force (purple), μ : Friction coefficient (red). The tests performed were

progressive linear scratch tests with the following load condition. Initial load was 0.3 mN, final load was 100 mN, the loading rate was 200 mN/min, and speed 2006 $\mu\text{m}/\text{min}$. The length of scratch was 1000 μm . The tests were performed at a temperature 24 $^{\circ}\text{C}$ with humidity conditions of 23 %RH

Integrity of nanostructured surfaces

A surface is able to meet the standards of a durable nanostructure when the surface structure adhesion is strong with the dense base material. Such adherence can be measured by a standard ASTM scratch test, such as the

ASTM E 2546 standard (also referred to as single point dynamic surface adherence test standard). This test involves an increasing load on a scratch-tip while it is translated on the surface. Strong adhesion is present for a nanostructured coating when (i) the surface does not delaminate even under a the high tip-load (100 mN), (ii)

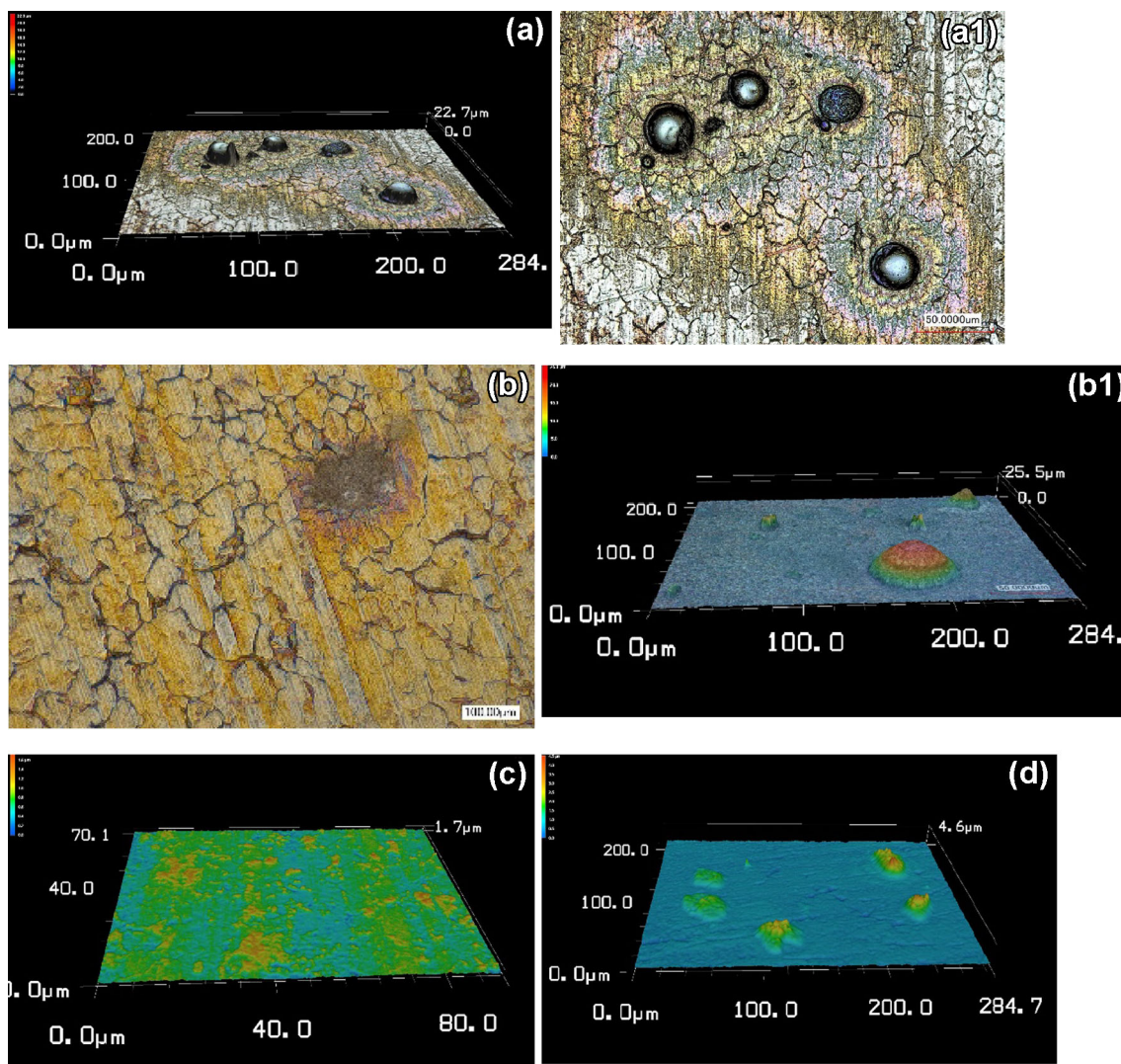


Fig. 4 Biofilm formation observations on nanostructured and virgin surfaces. **a** and corresponding **a1** are different views of the surface of a titanium nanostructured 304 stainless steel, inoculated with *Enterobacter aerogenes* and nutrient. The observation for **a** was made on a surface 7 years after the inoculation. Isolated bacterial colonies are noted, and the original grains are visible. **b** and corresponding **b1** are different views of a nano-MoS₂ on SS 316 substrate, inoculated with *Bacillus Cereus* and observed after 3 years. Both **a**, **b** show that the surface, after many years, displays sporadic colony like features that are of micron-scale size (~50 microns). No colony growth was noted in a corresponding 24 h. AOAC test on either surface, indicating that the surfaces had reduced their bacterial concentrations. Note that the original grain structure is still seen in **a**, **b**. (i.e., most of the surface has not been covered by any film). **c** shows what is

possibly an airborne biofilm on the SS 316 after only 2 months of exposure—in this case, only nutrient was added with a swab with no bacterial species being introduced. A varying thickness of a biofilm layer is seen on the surface. Note that substrate grains are not visible in this figure, indicating a full biofilm coverage. **d** shows a micrograph from the same stainless steel substrate after 12 months. For this surface, the nutrient was added with a swab but no bacterial inoculants were introduced. Again, a varying thickness biofilm layer is noted on the surface. Also note that substrate grains are no longer visible, thus indicating a wide biofilm coverage. The surfaces were all left in a non-sterile laboratory environment (same as in Fig. 1). The SS316L grain size is about ten microns, and the SS304 has an average grain size of about 35 microns. Reddy et al. 2015a, b

the coatings display no cracks in the scratch, (iii) the coatings do not visibly chip-off, and; (iv) when the nanostructure substrate behaves in a ductile-manner, scratch behavior of the metallic substrate below the coating/nanosurface. We note here that the exact demarcation between the nanoporous part and the dense base may not be clearly demarcated. Features of good scratch-test results from silver nanostructure and molybdenum disilicide nanostructure are shown in Fig. 3. Scratch test results from Silver and molybdenum disilicide nanostructures are shown in Tables 1 and 2. Both the nanolayers are noted to be strongly adherent to the substrate, i.e., the 316 stainless steel. The corresponding scratch surface pictures, also shown in the table, show no delamination, lateral cracks, forward chevron tensile cracks, arc tensile cracks, hertzian tensile cracks, conformal cracks or buckling cracks. Additionally, no buckling spallation, wedging spallation, recovery spallation, gross spallation or chipping are noted. In a final assessment, an acoustic emission result also did not indicate any delamination.

Nanoporous structures are also produced by diffusion process based on the principle of Kirkendall effect. Such diffusion enabled nanopores are also very strongly bonded to the matrix. When two solids diffuse into each other at vastly different rates, a large number of vacancies are created leading to formation pore diameters in the nanoscale. For example, when zinc and copper are coupled there is an emergence with time of nanoporosity because the zinc has a very high diffusion coefficient in copper compared to copper in zinc. As a result, a large amount of zinc diffuses into the copper while a very small amount of copper diffuses into the zinc, thereby leading to the formation and coagulation of vacancies in zinc. Over time, by controlling the temperature and time, a desired nanostructures size may be promoted. Applications of such nanostructures include drug delivery systems, optics, electronics, and catalyst, and selective chemical reactors. Nanoporous and microporous structures are also produced by aqueous anodizing. During the past decade there has been some focus on the synthesis of nanoporous single crystal silicon wafers by this method. The silicon wafer is as the anode and dilute hydrofluoric acid is used as electrolyte. Nanoporous and microporous silicon are expected to also absorb more light and thus expected to increase the energy efficiency in solar applications. It is likely that this increased absorption extends to the ultra violet region with the higher energy frequencies. In this manner such surfaces may be expected to enhance antimicrobial impact.

In natural environments including that of laboratory air, microbes often form biofilms on solid surfaces. The microbes in a biofilm are thought to be held together with polysaccharides. Rod and fiber-like morphologies are commonly noted for biofilms (Reddy et al. 2012; Willey

et al. 2008) that are seen on stainless and other steels. Figure 4a–e from Reddy et al. 2012 shows results from a titanium nanostructure surface on stainless SS304 and SS316. The figures are taken at a magnification that reveals that the grain structures (i.e., the critical micron size features that are used for the steel specification) of the two stainless steels. This grain structure remains clearly visible for the surfaces where biofilms do not form even after 7 years, whereas without, the biofilms form easily within a month and rapidly grow, e.g., on the control surface, especially when polysaccharide availability is ensured at the beginning of a test (Reddy et al. 2012).

Correlations with drying and spreading

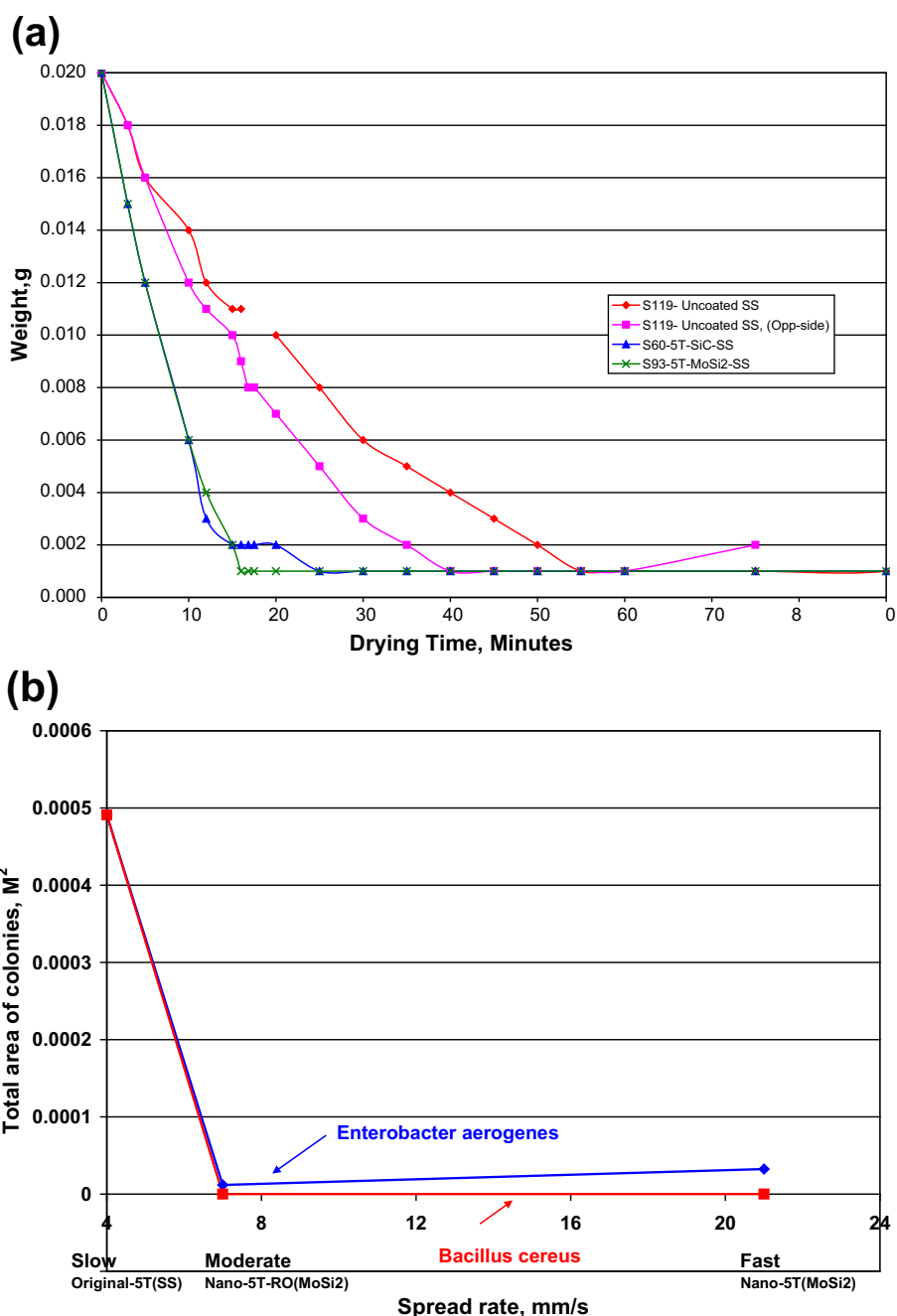
Based on only the few published results available in the literature, it appears that a high drying rate corresponds to a low contact angle for a droplet of water (and to good antimicrobial efficacy) on a surface (Reddy et al. 2012). These results are reproduced in Fig. 5. A much faster water drying rate is observed on surfaces that were coated with the MoSi_2 or Ag nanostructures containing the nanopores, when compared with uncoated stainless steel substrates (i.e., without the nanostructure coating).

Water droplet spread rates were characterized as slow, moderate and fast and also correlated with antimicrobial efficacy. The spread rate is measured by dropping 0.020 ± 0.005 g weight distilled-water droplet on the surfaces from a height of about 3–5 mm with a stopper and measuring the change in diameter of the droplet within one second. The spread rate that is noted for nanostructured porous surfaces was considerably higher than the surfaces without the nanoporous structure. A high drying rate and a high droplet spread rate appear to correlate well with antibacterial efficacy. These results are shown in Table 3.

Cascade e-ion nanostructuring

Nanopores and nanoscale microstructures are associated with diffuse interfaces. The maximum entropy production rate principle (MEPR) appears to have wide applicability for determining the curvature (shape) of microstructures that display diffuse interfaces. The modern theoretical foundations for determining and predicting the morphological stability of nano- and micron-level structures have only recently become available (Mińkowski et al. 2016; Bensah and Sekhar 2016). In time, these new models will undoubtedly be extended to provide greater predictability of all morphological features that can be formed even from complex non-equilibrium ion-processing methods (Sekhar 2015).

Fig. 5 a Drying rate studies indicate that the drying rate (initial slope) of nanostructured surfaces is considerably faster than the control surfaces. Room temperature 19 °C (66 F), with 45 % relative humidity. The surfaces labeled—5T were nanostructures of SiC and MoSi₂. **b** Bacterial activity (total area of colonies developed in 24 h.) versus spread rate of a water droplet on a similarly constructed surface for Gram positive and negative representative species. (Reddy et al. 2012.) Note that the surfaces labeled “Nano” showed a higher spread rate and strong antibacterial behavior. Note from **a** that these surfaces also tended to dry faster

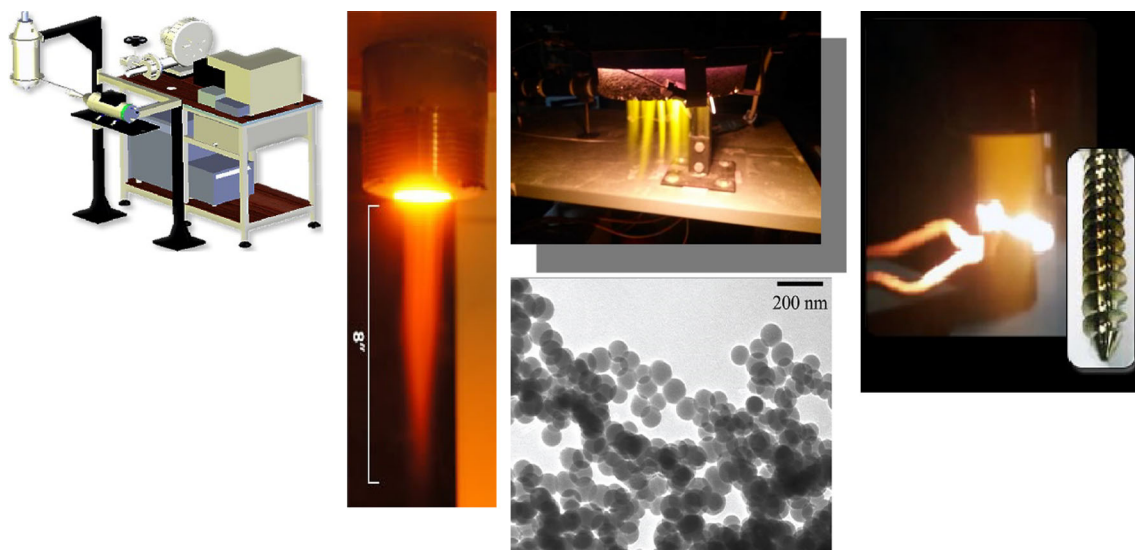


An air plasma technique for creating hard, durable and low-wear nanosurface nanocrystal formation has recently become commercial. This is known as the cascade e-ion method. In this method, extremely rapid, ion-assisted growth conditions are possible (Rajamani 2006), with which nanosurface structures may be created and manipulated within a few seconds. The cascade-treated surfaces show low wear (because of hard oxynitride formation) and additionally appear to show antimicrobial properties (Table 3). The technique allows for tuning the surface for variations in the surface dopant concentrations. The

cascade e-ion machine is shown schematically in Fig. 6a. The various plume possibilities are shown in Fig. 6b, c. Plumes are varied for in situ growth or plasma deposition. A picture of a biomedical screw undergoing surface treatment by immersing in the beam is shown in Fig. 6d. Perfectly formed round glass nanobeads shown in Fig. 7b are possible for nanodeposits. This cascade e-ion process is reported to only add a cost of <2 US cents per part (www.mhi-inc.com), thus making it possibly the preferred industrial technique for nanostructuring. Large and small engineering product surfaces are easily treated with

Table 3 Bacterial recovery and corresponding water droplet test on cascade e-ion modified surfaces

Condition	Contact (Residence) time prior to test (min)	RFU measured after contact	Drying rate	Remarks
Untreated (control)	0	2419	Medium	As obtained roller finished 316 stainless steel
Five seconds beam exposure to a nitrogen-enriched beam.	30	665–716	Rapid	Sand blasted and cascade e-ion-exposed stainless steel 316 alloy
Thirty-second air ion beam exposure in the cascade e-ion beam	30	603–622	Rapid	Sand blasted and cascade e-ion-exposed stainless steel 316 alloy. XPS confirmed nitrogen and oxygen peaks. EDAX confirmed iron oxynitrides
Thirty-second air and steam ion beam exposure in the cascade e-ion beam	30	799–849	Medium	Sand blasted and cascade e-ion-exposed stainless steel 316 alloy. XPS confirmed nitrogen and oxygen peaks. EDAX confirmed iron oxynitrides
Light layer silver nanosurface in air/steam ions of cascade e-ion	40	756	Rapid	Cascade e-ion-exposed stainless steel 316 alloy with the light layering. No sand blasting
Thirty-second exposure to an air/steam cascade e-ion beam	40	1343	Slow	Cascade e-ion-exposed stainless steel 316 alloy. No sandblasting. XPS confirmed nitrogen and oxygen peaks. EDAX confirmed iron oxynitrides
2.5-min exposure to air/steam ions of the cascade e-ion. Light layering of Hafnium oxide mode	40	1673	Slow	Cascade e-ion-exposed stainless steel 316 alloy with the light layering

**Fig. 6** Schematic and beam photographs of the cascade e-ion. Depicted from *left to right* is a schematic of the full machine, the various beam possibilities and nanodeposits, and a picture of a titanium biomedical-use screw being treated in the beam

the cascade e-ion technique because the beam does not need to be enclosed in a chamber. Nitrides and oxynitrides are formed by air plasma or air/steam plasma on most surfaces exposed to the Cascade e-ion plasma beam.

The ability of predictively tuning the functional properties of nanocrystals by changing the shape of the nanostructures is an important possibility for future requirements for the antimicrobial action from

nanostructures (Laurikaitis et al. 2008; Carvalho et al. 2013). The surface nanostructure formation sequence described in (Mittemijer 2013) is reproduced in Fig. 7b and is perhaps one the few current example which pictorially describes the morphological nanofeature evolution in a surface microstructure. Oxynitrides are particularly suitable for any tunability as they offer easy band gap variations that arise from the changes in the surface N/O element ratio (Vasconcellos et al. 2010; Kar et al. 2015;

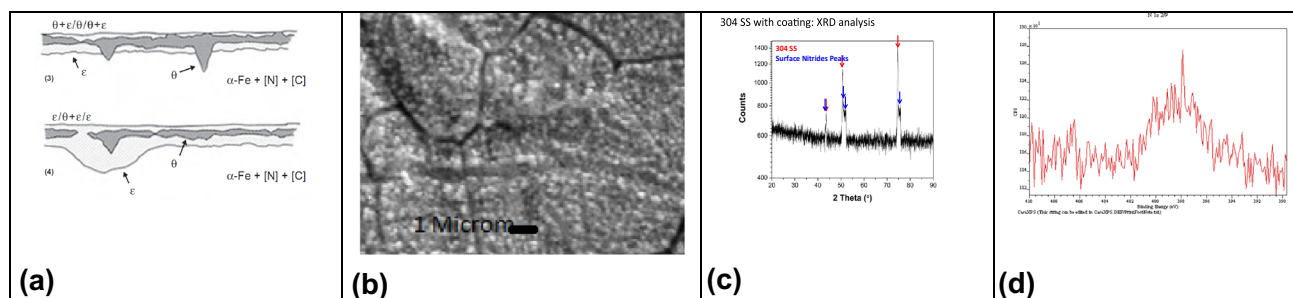


Fig. 7 Typical nanostructures formed on a stainless steel surface exposed to the cascade e-ion beam for about fifteen seconds. **a** Surface nanostructure evolution sequence proposed in Mittermijer 2013,

Feng et al. 2012). Additional theoretical work is required for incorporating nanoporous features. Some magnified views of the observed nanograins and, nanoparticles on 304 stainless, made with the cascade technique are shown in Fig. 7c, d. An XPS signature from the nitrogen binding-energy peaks that are observed in steel, titanium and zirconium surfaces after brief exposure to the cascade e-ion beam is shown in Fig. 7e. Table 3 compares the RFU recovery on surfaces exposed to the cascade e-ion along with corresponding water drying rates (see Fig. 5 above for details) observed on identical surfaces. These results appear to correlate well with the results reported in the literature (Reddy et al. 2012).

Summary

There is by now considerable evidence that nanoporous nanostructured surfaces offer the possibility of permanent antimicrobial properties. Yet it is clear that more research is required. Nanoporous surfaces may be employed in several ways; as a reservoir for chemicals or without the need of chemicals by exploiting the topology of the nanoporous nanostructure. The few available correlations with a water droplet spread rate, surface drying rate and the antimicrobial efficacy are reviewed. These simple tests present a possible quick analysis of the efficacy. Discussions are also provided for the fundamental understanding of the morphological evolution possibilities for the formation of the internal structure of a nanoporous coating or an in situ grown surface layer. An air plasma method for nanoporous nanostructuring is discussed.

Acknowledgments The research reported in this article was performed with combined funding from various sources. An MHI-EPA CRADA #682-12 with The US Environmental Protection Agency, ORD, NRMRL, WSWRD, 26 W. Martin Luther King Dr. Cincinnati, OH, 45268, USA is acknowledged which enabled use of the MHI cascade e-ion. The authors gratefully acknowledge NSF funding (GS), EPA funding (NM) and considerable considerations provided by Micropyletics Heaters International Inc. (MHI Inc.) from corporate R&D funds #MHI3-4/205-2016. Scratch tests were performed at CSM laboratories.

b surface nanostructures formed on Cascade e-ion treated SS304, **c** X-ray diffraction peaks of Oxynitride on SS 304, **d** XPS nitrogen signature on SS304 exposed to the cascade e-ion

Trade Names The trade name cascade e-ion and PermaClean S-e-ion-10 belong to Micropyletics Heaters International Inc. USA. The luminosity meter is manufactured by Kikkoman Japan, model number Luminester PD-20.

References

- AOAC Official Methods of Analysis (1988) 18 Chapter 17, pp 10, 1995 Cited from Journal AOAC, 343
- Atha DH, Wang H, Petersen EJ, Cleveland D, Holbrook RD, Jaruga P, Dizdaroglu M, Xing B, Nelson BC (2012) Copper oxide nanoparticle mediated DNA damage in terrestrial plant models. *Environ Sci Technol* 46:1819–1827
- Bacakova L, Svorcik V (2008) Cell colonization control by physical and chemical modification of materials. In: Kimura D (ed) *Cell Growth processes: new research*. Nova Science Publishers Inc., New York, pp 5–56
- Bensah YD, Sekhar JA (2016) <http://arxiv.org/abs/1605.05005>
- Boccaccini AR, Höland W (2016) Editorial: Inorganic Biomaterials. *Front Bioengineering Biotechnol* 4
- Burada V, Sekhar JA, Batt J, Reddy GS, Kandell B (2014) US Patent 8895888
- Cafun JD, Kvashnina KO, Casals E, Puentes VF, Glatzel P (2013) Absence of Ce³⁺ sites in chemically active colloidal ceria nanoparticles. *ACS Nano* 7:10726–10732
- Carvalho P, Cunha L, Barradas NP, Alves E, Espinos JP, Vaz F (2013) Tuneable properties of zirconium oxynitride thin films. In: *Metallic oxynitride thin films by reactive sputtering and related deposition methods: process, properties and applications*, vol 49, pp 64–112
- Child T (2006) Antimicrobial surfaces in the food industry. *New Food Mag*, issue 2. <http://www.newfoodmagazine.com/2071/new-food-magazine/past-issues/antimicrobial-surfaces-in-the-food-industry/>
- Chung CJ, Lin HI, He JL (2007) Antimicrobial efficacy of photocatalytic TiO₂ coatings prepared by arc ion plating. *Surf Coat Technol* 202:1302–1307
- Coleman WH, Setlow P (2008) Analysis of damage due to moist heat treatment of spores of *Bacillus subtilis*. *J Appl Microbiol* 1–8. ISSN 1364-5072
- Connelly MC, Dismukes JP, Sekhar JA (2012) New relationships between production and patent activity during the high-growth life cycle stage for materials. *Technol Forecast Soc Chang* 78(2):303–318
- Cortezzo DE, Koziol-Dube K, Setlow B, Setlow P (2004) Treatment with oxidizing agents damages the inner membrane of spores of *Bacillus subtilis* and sensitizes spores to subsequent stress. *J Appl Microbiol* 97:838–852

- Cvetkovic A, Meno AL, Thorgersen MP, Scott JW, Poole FL, Jenney FE Jr, Lancaster A, Praissman JL, Shanmukh S, Vaccaro BJ, Trauger SA, Kalisiak E, Apon JV, Siuzdar G, Yannone SM, Tainer JA, Adams MWW (2010) Microbial metalloproteomes are largely uncharacterized. *Nature* 466:779–782
- Dai L, St. John HAW, Bi J, Zientek P, Chatelier RC, Griesser HJ (2000) Biomedical coatings by the covalent immobilization of polysaccharides onto gas-plasma-activated polymer surfaces. *Surf Interface Anal* 29:46–55
- de la Fuente D, Diaz I, Simancas J, Chico B, Morcillo M (2010) Long-term atmospheric corrosion of mild steel. *Corros Sci* 53:604–617
- Emerson D, Moyer C (1997) Isolation and characterization of novel iron-oxidizing bacteria that grow at circum neutral pH. *Appl Environ Microbiol* 63:4784–4792
- Feng J, Slocik JM, Sarikaya M, Naik R, Farmer BL, Heinz H (2012) Influence of the shape of nanostructured metal surfaces on adsorption of single peptide molecules in aqueous solution. *Small*. doi:10.1002/sml.201102066
- Finneran KT, Johnsen CV, Lovley DR (2003) *Rhodoferrax ferrireducens* sp. Nov., a psychrotolerant, facultatively anaerobic bacterium that oxidizes acetate with the reduction of Fe(III). *Int J Syst Evol Microbiol* 53:669–673
- Fontana MG, Green ND (1967) Green, corrosion engineering. McGraw-Hill, New York
- Graff M, Seifert O (2005) ALWC on a jetty: a case history from discovery to repair. In: Second international conference on accelerated low water corrosion held at Liverpool, England
- Hamilton WA (1985) Sulfate-reducing bacteria and anaerobic corrosion. *Ann Rev Microbiol* 39(195–217):1985
- Heitz E, Flemming HC, Sand W (1996) Microbially influenced corrosion of materials. Springer, Berlin
- Hicks RE (2009) Assessing the role of microorganisms in the accelerated corrosion of port transportation infrastructure in the Duluth-Superior Harbor. CURA Report 1–10
- Japanese Industrial Standard: JIS Z 2801: 2000, 1.0 (2005), pp 1–3
- Javaher R (2008) Microbiologically influenced corrosion—an engineering insight. Springer, Berlin
- Kar A, Sain S, Kundu A, Bhattacharyya A, Pradhan SK, Patra A (2015) Influence of size and shape on the photocatalytic properties of SnO₂ nanocrystals. *Chem Phys Chem* 16:1017–1025. doi:10.1002/cphc.201402864
- Keough B, Schmidt TM, Hicks RE (2003) Archaeal nucleic acids in picoplankton from great lakes on three continents. *Microb Ecol* 46:238–248
- Ketabchi A, Komm K, Miles-Rossouw M, Cassani AD, Variola F (2016) Nanoporous titanium surfaces for sustained elution of proteins and antibiotics. *PloS One*. doi:10.1371/journal.pone.0092080
- Kobrin G (1993) A Practical manual on microbiologically influenced corrosion. NACE, Houston
- Ksoll WB, Ishii S, Sadowsky MJ, Hicks RE (2007) Presence and sources of fecal. Coliform bacteria in epilithic periphyton communities of lake superior. *Appl Environ Microbiol* 73:3771–3778
- Lam CW, James JT, McCluskey R, Hunter RL (2004) Pulmonary toxicity of single-wall carbon nano-tubes in mice 7 and 90 days after intratracheal instillation. *Toxicol Sci* 77:126–134
- Lane DJ (1991) 16S/23S rRNA sequencing in nucleic acid techniques in bacterial systematics. Wiley, New York, pp 115–175
- Laurikaitis M, Burinskas S, Dudonis J, Mileius D (2008) Physical properties of zirconium oxynitride films deposited by reactive magnetron sputtering. *J Phys Conf Ser* 100:082051. doi:10.1088/1742-6596/100/8/082051
- Li HP, Bhaduri SB, Sekhar JA (1992) Metal matrix composites based on the Ti–B–Cu-porosity system. *Metall Trans A* 23(1):251–261
- Li Z, Lee D, Sheng X, Cohen RE, Rubner MF (2006) Two-level antibacterial coating with both release-killing and contact-killing capabilities. *Langmuir* 22:9820–9823
- Liao KH, Ou KL, Cheng H, Lin CT, Peng PW (2010) Effect of silver on antibacterial properties of stainless steel. *J Appl Surf Sci* 256(11):1–5
- Locklin J (2011) A new anti-microbial treatment that can make clothing—including smelly socks—permanently germ-free. *ACM J Appl Mater Interfaces*
- Losic D, Santos A (2015) Electrochemically engineered nanoporous materials. Springer, Berlin. ISBN: 3319203454
- Marsh CP, Bushman J, Beitelman AD, Bucheit RG, Little BJ (2005) Freshwater corrosion in the Duluth-Superior Harbor—summary of the initial workshop findings. Special Publication ERDC/CERL SR-05-3, U.S. Army Corps of Engineers
- Mayhall CG (1999) Hospital epidemiology and infection control, 2nd edn. Lippincott Williams and Wilkins, Philadelphia
- Michels HT, Noyce JO, Keevil CW (2009) Effects of temperature and humidity on the efficacy of methicillin-resistant *Staphylococcus aureus* challenged antimicrobial materials containing silver and copper. *Lett Appl Microbiol* 49:191–195
- Mińkowski M, Zaluska-Kotur MA, Turski LA, Karczewski G (2016) <http://arxiv.org/abs/1605.07820>
- Mittemijer EJ (2013) Fundamentals of nitriding and nitrocarburizing. ASM Handbook, Steel Heat Treating Fundamentals and Processes, vol 4, pp 619–631
- Moseneder MM, Arrieta JM, Muiyzer G, Winter C, Herndl GJ (1999) Optimization of terminal-restriction fragment length polymorphism analysis for complex marine bacterioplankton communities and comparison with denaturing gradient gel electrophoresis. *Appl Environ Microbiol* 65:4333–4339
- Noyce JO, Michels HT, Keevil CW (2006) Potential use of copper surfaces to reduce survival of epidemic methicillin-resistant *Staphylococcus aureus* in the healthcare environment. *J Hosp Infect* 63:289–297
- Noyce JO, Michels HT, Keevil CW (2007) Inactivation of influenza A virus on copper versus stainless steel surfaces. *Appl Environ Microbiol* 73(8):2748–2750
- Örnek D, Wood TK, Hsu CH, Mansfeld F (2002) Corrosion control using regenerative biofilms (CCURB) on brass in different media. *Corros Sci* 44(10):2291–2302
- Rahman M, Duggan P, Dowling DP, Hashmi MSJ (2007) Continuously deposited duplex biomedical coatings. *Surf Coat Technol* 201:5310–5317
- Rajamani V, Anand R, Reddy GS, Sekhar JA, Jog MA (2006) Heat-transfer enhancement using weakly ionized, atmospheric pressure plasma in metallurgical applications. *Metall Mater Trans B* 37(4):565–570
- Rao TS, Sairam TN, Viswanathan B, Nair KVK (2000) Carbon steel corrosion by iron-oxidizing and sulphate reducing bacteria in a freshwater cooling system. *Corros Sci* 42:1354–1360
- Reddy GS, Nadagouda MN, Sekhar JA (2012) Innovation in materials science-2 key engineering materials, vol 521. Trans Tech Publishing, Switzerland, pp 1–41
- Reddy GS, Sekhar JA (2016) Antimicrobial materials and coatings. US Patent 9,376,771
- Reddy GS, Vissa R, Sekhar JA (2015) US Patent 8940245
- Reddy GS, Vissa R, Sekhar JA (2015) US Patent 8945468
- Santos GM, de Santi Ferrara FI, Zhao F, Rodrigues DF, Shih WC (2016) Photothermal inactivation of heat-resistant bacteria on nanoporous gold disk arrays. *Opt Mater Express* 6(4):1217–1229
- Sekhar JA (2015) Editorial overview: materials engineering: the shape of materials engineering for the next 100 years. In: Current opinion in chemical engineering. Elsevier, pp 2–9
- Sekhar JA, Mantri AS, Yamjala S, Saha S, Balamuralikrishnan R, Rao PR (2015) Ancient metal mirror alloy revisited: *quasicrystalline nanoparticles observed*. *JOM* 67:2976–2983

- Setlow P (2006) Spores of *Bacillus subtilis*: their resistance to and killing by radiation. *Heat Chem J Appl Microbiol* 101:514–525
- Service RF (2004) Nanomaterials show signs of toxicity. *Sci* 300, p 243
- Starovetsky D, Armon R, Yahalom J, Starovetsky J (2001) Pitting corrosion of carbon steel caused by iron bacteria. *Int Biodeterior Biodegrad* 47:79–87
- Tiller JC, Liao CJ, Lewis K, Klivanov AM (2001) Designing surfaces that kill bacteria on contact. *PNAS* 98:5981–5985. doi:[10.1073/pnas.111143098](https://doi.org/10.1073/pnas.111143098)
- Vasconcellos MAZ, Lima SC, Hinrichs R (2010) Hardness evaluation, stoichiometry and grain size of titanium nitride films obtained with plasma nitriding on Ti–6Al–4V samples. *Revsta Matér* 15:299–302
- Videla H (1996) *Manual of biocorrosion*. CRC Press, Boca Raton
- Visai L, De Nardo L, Punta C, Melone L, Cigada A, Imbriani M, Arciola CR (2011) Titanium oxide antibacterial surfaces in biomedical devices. *Int J Artif Organs* 9:929–946
- Willey J, Sherwood LM, Woolverton CJ (2008) *Microbiology*. McGraw Hill, ISBN: 0072992913, Chapter 5. www.mhi-inc.com. Accessed 2 April 2016
- Xu L, Takemura T, Cu M, Hanagata N (2011) Toxicity of silver nanoparticles as assessed by global gene expression analysis. *Mater Express* 1:74–79
- Yuan SJ, Pehkonen SO (2009) AFM study of microbial colonization and its deleterious effect on 304 stainless steel by *Pseudomonas NCIMB 2021* and *Desulfovibrio desulfuricans* in simulated seawater. *Corros Sci* 51:1372–1385